Manganese-doped yttrium orthoaluminate: A potential material for holographic recording and data storage

G. B. Loutts, M. Warren, L. Taylor, R. R. Rakhimov, H. R. Ries, and G. Miller III
Center for Materials Research, Norfolk State University, 2401 Corprew Avenue, Norfolk, Virginia 23504

M. A. Noginov,* M. Curley, N. Noginova,* N. Kukhtarev, H. J. Caulfield, and P. Venkateswarlu†
Center for Nonlinear Optics and Materials, Department of Physics, Alabama A&M University, P.O. Box 1268, Normal, Alabama 35672
(Received 18 August 1997; revised manuscript received 20 October 1997)

Optical properties of manganese-doped yttrium orthoaluminate crystals (Mn:$YAlO_3$), grown by the Czochralski technique, are reported. Luminescence and absorption spectra indicate the presence of Mn^{4+} ions in as-grown crystals, and Mn^{3+}, Mn^{4+}, and Mn^{5+} ions simultaneously in photoexcited crystals. A permanent diffraction grating, erasable by heating, was obtained in the crystals with diffraction efficiency of more than 50% at 514.5 nm reading wavelength and 1–2 % in 632–930 nm wavelength range. Reading at wavelengths longer than 630 nm did not damage the recorded grating. The electro-optical effect observed in the photoexcited crystals implies that manganese ions disturb the $YAlO_3$ crystal structure so that it becomes noncentrosymmetric. [S0163-1829(98)03804-1]

Oxide crystals doped with transition metal ions can exhibit optically induced changes of the refractive index (photorefractive effect). In some noncentrosymmetric crystals, for example, in ferroelectrics, photoelectrons are generated when light of suitable wavelength is incident on the crystal. The photoelectrons then migrate in the lattice and are subsequently trapped at new sites. The resulting space charge distribution gives rise to an electric-field grating which is a spatial derivative of the generic light intensity (nonlocal or diffusion-type nonlinearity[1]). This electric field grating induces a refractive-index (or holographic) grating via the linear electro-optical effect. In centrosymmetric crystals, local changes in the refractive index are possible due to photoinduced oxidation-reduction effects accompanied by the color changes. In some doped insulators, such as ruby, large optical nonlinearities can result from excited state population changes and the difference in the susceptibility between the ground and metastable states levels in the optically pumped material.[2] A beam coupling gain of 22 for a weak probe laser beam using a moving grating technique[3] and self-oscillation based on this gain[4] have been obtained in Cr^{3+} doped yttrium orthoaluminate (Cr:$YAlO_3$). The above was a motivation for us to introduce Mn^{4+} ions in $YAlO_3$ crystals and study their nonlinear optical properties. Since Mn^{4+} has the same d^3 electron configuration as Cr^{3+} but is less stable and can transform to other valence states,[5] we expected that both color changes and population changes might be optically induced.

Yttrium orthoaluminate or $YAlO_3$ has a distorted perovskite structure that belongs to the orthorhombic centrosymmetric *Pbnm* space group.[6] There are two kinds of cationic sites in the structure available for Mn substitution: relatively large, strongly distorted YO_{12} polyhedra (Y^{3+} ionic radius $R_Y = 1.02$ Å) and smaller, nearly ideal AlO_6 octahedra ($R_{Al} = 0.53$ Å). Manganese may enter the $YAlO_3$ host in the form of Mn^{2+} ions ($R_{Mn} = 0.96$ Å), substituting most likely Y^{3+} ions; and Mn^{3+} ions ($R_{Mn} = 0.65$ Å) or Mn^{4+} ions ($R_{Mn} = 0.53$ Å), substituting Al^{3+} ions. The last substitution is most probable in terms of the dimensional criterion. Cation vacancies, which are common in $YAlO_3$ crystals grown in oxygen-containing atmosphere,[7] may provide the charge compensation required for Mn^{4+} substitution.

Mn:$YAlO_3$ crystals were grown by the conventional Czochralski technique in a 3 in. iridium crucible under nitrogen ambient atmosphere with up to 0.5% of oxygen. 99.999% purity chemicals were used for the charge preparation. Manganese was introduced in the melt at 0.05–2.0 at. % (with respect to Al) in the form of MnO_2. The seed was oriented in the *b* direction of the orthorhombic unit cell, the pull rate was maintained at 1.5 mm/h and the rotation rate at 15 rpm.

As-grown Mn:$YAlO_3$ crystals did not contain any visible defects except for a very thin core with bubbles or black inclusions in the bottom part. Even a small addition of Mn (as low as 0.05%) removed the red-brown cast characteristic of undoped $YAlO_3$ crystals grown in a nitrogen/oxygen environment. Instead, Mn doping produced a clean yellow color in both neutral and oxidizing atmospheres.

Lattice parameters of Mn:$YAlO_3$ crystals were determined by x-ray powder diffraction. An undoped $YAlO_3$ crystal had the lattice parameters of $a = 5.178(1)$ Å, $b = 5.328(1)$ Å, and $c = 7.367(1)$ Å. In Mn-doped crystals all the lattice parameters were decreased. In particular, $a = 5.169(2)$ Å, $b = 5.317(2)$ Å, and $c = 7.354(3)$ Å were obtained in a 0.5% Mn:$YAlO_3$ sample. The manganese concentration in the crystals, determined by electron microprobe analysis, was 10–12 times lower than that in the melt. This implies that the distribution coefficient of Mn (K), which is a ratio of Mn concentration in the crystal and Mn concentration in the melt, is less than 0.1. However, the distribution of Mn within the crystals was much more uniform than it might be expected with $K = 0.1$. The theoretical distribution of a nonvolatile impurity in a Czochralski-grown crystal is given by $C = KC_0(1-g)^{K-1}$, where C is the concentration of impurity in the crystal when the fraction of melt crystallized is

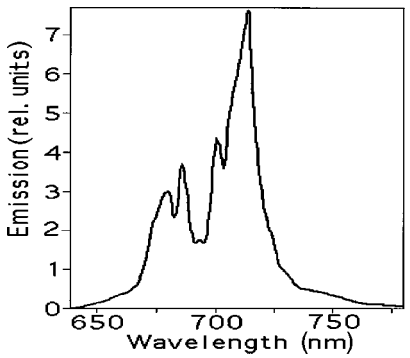

FIG. 1. Room temperature emission spectrum of Mn:$YAlO_3$.

g, and C_0 is the initial concentration of impurity in the melt.[8] We measured the concentration of Mn in the top ($g=0.01$) and bottom ($g=0.37$) parts of a Mn:$YAlO_3$ crystal and obtained $K=0.55$, using the above equation. Apparently, the incorporation of manganese in the $YAlO_3$ host was limited not only by its concentration in the melt. Another factor was the concentration of intrinsic defects that provided the charge compensation for Mn^{4+} ions substituting Al^{3+} ions.

The unpolarized emission spectrum of Mn:$YAlO_3$ is shown in Fig. 1. It consists of four distinguishable peaks centered at 682, 689.5, 703, and 715 nm and has the same shape in all the samples, both at Q-switched 532 nm and cw 488 nm excitation. Similar luminescence, observed in Mn-doped α-Al_2O_3,[9] $LaAlO_3$,[10,11] and YAG[5,12,13] has been unambiguously attributed to the ^2E-$^4A_2$ transition of Mn^{4+} ions. The room-temperature luminescence kinetics was close to single exponential with decay times of 2.57–2.83 ms, depending on Mn concentration. The decay time was the same in all four emission peaks. As far as we know, this is the longest decay time registered in Mn^{4+}-doped crystals, implying efficient energy storage in the material.

The unpolarized optical absorption spectrum of an as-grown Mn:$YAlO_3$ sample is shown in Fig. 2, curve 1. The absorption band centered at 480 nm is due to transitions from the ground $^4A_2$ state to the first excited quartet state $^4T_2$. The very strong band at 290 nm can be attributed to the superposition of the $^4A_2$-$^4T_1$ transition of Mn^{4+} ions and a charge transfer band.[5,9,11,13]

Electron paramagnetic resonance (EPR) spectra of Mn:$YAlO_3$ powder samples were recorded with an X-band EMX Bruker spectrometer at room temperature. In such a setup, two types of paramagnetic centers, Mn^{2+} ions, $S=\frac{5}{2}$, and Mn^{4+} ions, $S=\frac{3}{2}$ can be registered. Mn^{2+} ions were identified in all samples, although no correlation was detected between the EPR signal and optical emission or absorption spectra. The intensity of a relatively weak EPR signal, associated with Mn^{4+} ions, was found to directly correlate with the optical absorption at 480 nm. A detailed analysis of the EPR data will be reported in a separate paper.

An Ar^+ laser illumination produced deep bluish-gray coloration in the yellow Mn:$YAlO_3$ samples. Absorption spectra of a 0.5% Mn:$YAlO_3$ sample obtained at different doses of laser radiation are shown in Fig. 2, curves 2 and 3. The infrared absorption extends up to 1.5 μm. According to the published spectroscopic data on different Mn ions[5,14] and

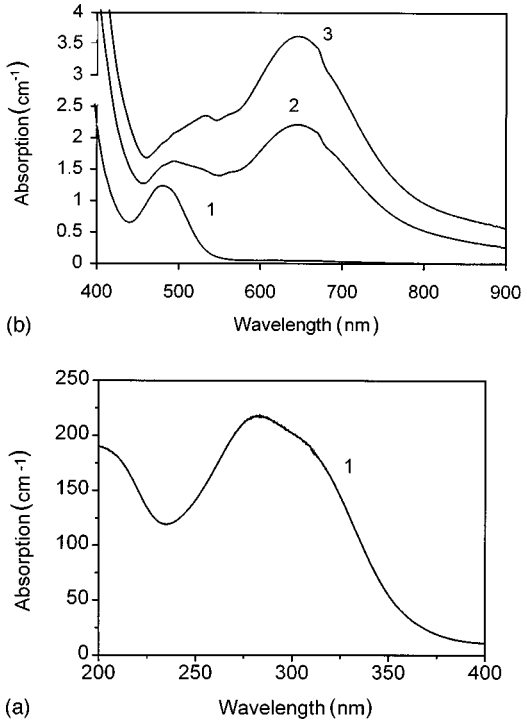

FIG. 2. Room temperature UV (a) and VIS-IR (b) absorption spectra of a 0.5% Mn:$YAlO_3$ crystal: as-grown (1); exposed to a medium dose of Ar^+ laser radiation (2), exposed to a high dose of Ar^+ laser radiation (3).

other transition metal ions with d^2 electron configuration,[15] the absorption feature at 530 nm can be assigned to the ^5E-$^5T_2$ transition in Mn^{3+} ions, and the strong and broad band, peaked at 650 nm, to the $^3T_1(t_2^2)$-$^3T_2(t_2e)$ transition in Mn^{5+} ions. Apparently, the optical excitation induces a reversible disproportionation reaction $2Mn^{4+} \Leftrightarrow Mn^{3+} + Mn^{5+}$ in $YAlO_3$. Absorption of all three ion species produces the gray coloration. The maximum photoinduced coloration at 650 nm was found to be proportional to the initial concentration of Mn^{4+} ions. At room temperature, 10% of the coloration was bleached within a day, however, around 50% of it remained in the sample for more than a year. Annealing at temperature higher than 250 °C completely bleached the sample in less than half an hour. Orange thermoluminescence was observed during the annealing.

In the holographic diffraction experiments, schematically shown in Fig. 3, a 0.5% Mn:$YAlO_3$ sample was illuminated

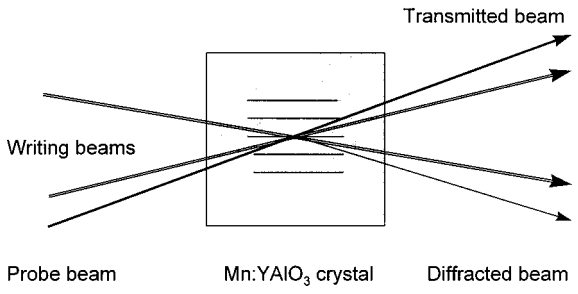

FIG. 3. Schematic diagram of the diffraction measurements setup.

with two mutually coherent, vertically polarized Ar^+ laser beams (514.5 nm) crossing at an angle of 0.01–0.025 rad. The sample was oriented such that its front face contained the *a* and *c* axes of the orthorhombic unit cell, with the *c* axis being horizontal. An energy exchange between the writing beams was observed during the grating recording, the effect characteristic of photorefractive crystals with nonlocal holographic response. In particular, the ratio of the intensities of two transmitted beams changed from unity to more than five during the grating recording. When the sample was rotated by 180° about its horizontal axis, the direction of energy exchange reversed. The recorded grating was probed with Ar^+ laser, He-Ne laser, and Ti-sapphire laser beams each coming to the sample at the Bragg angle. The ratio of intensity of the diffracted beam to intensity of the diffracted and transmitted beams combined was as large as 53% at 514.5 nm wavelength. In different orientations of the sample the diffraction efficiency varied from around 1 to 50 %. The theoretical limit of diffraction on absorption grating is 3.7%,[16] so we explain the high diffraction efficiency mainly by diffraction on the refractive index grating, with possible small contribution from the absorption. The highest diffraction efficiency calculated relative to the incident light intensity was 1.2% at 632.8 nm, 2.1% at 800 nm, and 1.1% at 930 nm. The He-Ne and Ti-sapphire probe beams of 50 mW power did not produce any additional coloration and did not disturb or erase the recorded grating, implementing a nonvolatile reading.

Under excitation of the sample with green light, the diffraction signal increased in time, reached the maximum, and then slowly decayed, Fig. 4, inset. The decay of diffraction signal can be explained by a combination of two reasons: (1) saturation of the grating due to exhaustion of Mn^{4+} concentration in the peaks of illumination and/or (2) build-up of Mn^{5+} absorption that reduced the intensity of the transmitted probe light. Both the rate of the coloration build-up and rate of the diffracted beam intensity build-up were found to be proportional to the incident beam intensity squared. This indicates that the photoinization by green light is a two-photon process.

The presence of energy exchange between writing beams and, hence, electro-optical effect in photoexcited Mn:$YAlO_3$ imply that the crystal is not centrosymmetric, contrary to undoped $YAlO_3$. Transitions from centrosymmetric to noncentrosymmetric phases have been observed in many ferroelectric crystals with the perovskite structure. Usually such

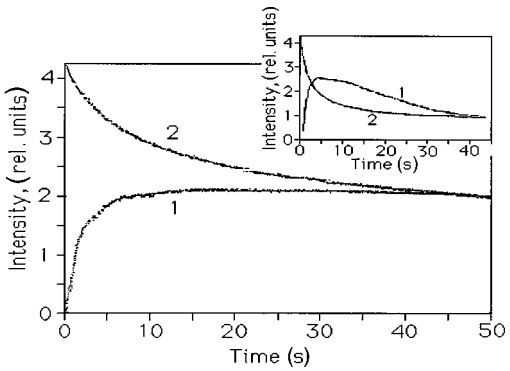

FIG. 4. Dynamics of diffracted (1) and transmitted (2) He-Ne beams in a 0.5% Mn:$YAlO_3$ sample excited with two mutually coherent 514.5 nm laser beams with the intensity in each of 2.1 J/cm^2 in the main frame and 4.2 J/cm^2 in the inset. Curves 1 and 2 are drawn not to scale.

transitions occur upon cooling the crystals below the Curie temperature. In $BaTiO_3$ the transition is accompanied by a shift of Ti^{4+} ions from the center of the octahedral position in the direction of the apical oxygen.[17] This gives rise to a spontaneous polarization. In Mn:$YAlO_3$ the symmetry disturbance may be due to a similar displacement of Mn ions from the center of the Al octahedral position. Since Mn^{3+} and Mn^{4+} are, respectively, larger or equal in size to Al^{3+} ions, it is more likely that much smaller Mn^{5+} ions are capable of such a displacement.

A high potential of Mn:$YAlO_3$ for applications in holography and optical storage is demonstrated by the high diffraction efficiency obtained in the visible and near infrared regions, combined with the high stability of the recorded grating at room temperature and its easy removal at elevated temperatures. More experimental and theoretical studies are needed for better understanding of the mechanisms of photoionization and diffraction, as well as for optimization of the crystal properties for different applications.

The authors would like to thank S. V. Lavrishchev for the electron microprobe analysis of Mn:$YAlO_3$ samples. Support for the work was provided by NASA Grant No. 92-207 and U.S. DOE Grant No. DE-FG01-94EW11493 at Norfolk State University; and by ONR/BMDO Grant No. N00014-96-1-5015 and NSF Grant No. HRD-9353548 at Alabama A&M University.

*Present address: Center for Materials Research, Norfolk State University, 2401 Corprew Avenue, Norfolk, Virginia 23504.

†Deceased.

[1] N. Kukhtarev, V. Markov, S. Odulov, M. Soskin, and V. Vinetskii, Ferroelectrics **22**, 949 (1979).

[2] P. Liao and D. Bloom, Opt. Lett. **3**, 4 (1978).

[3] I. McMichael, R. Saxena, T. Chang, Q. Shu, S. Rand, J. Chen, and H. Tuller, Opt. Lett. **19**, 1511 (1994).

[4] I. McMichael, T. Y. Chang, M. A. Noginov, M. Curley, P. Venkateswarlu, and H. Tuller, *OSA Trends in Optics and Photonics on Advanced Solid State Lasers*, edited by Stephen A. Payne and Clifford R. Pollock (Optical Society of America, Washington, DC, 1996), Vol. 1, p. 569.

[5] K. Peterman and G. Huber, J. Lumin. **31/32**, 71 (1994).

[6] R. Diehl and G. Brandt, Mater. Res. Bull. **10**, 85 (1975).

[7] P. Dorenbos, M. V. Korzhik, A. P. Kudryavtseva, S. V. Lyubetskii, B. I. Minkov, V. B. Pavlenko, and A. A. Fyodorov, J. Appl. Spectrosc. **59**, 633 (1993).

[8] W. G. Pfann, *Zone Melting* (Wiley, New York, 1966).

[9] S. Geschwind, P. Kisliuk, M. P. Klein, J. P. Remeika, and D. L. Wood, Phys. Rev. **126**, 1684 (1962).

[10] Z. N. Zonn, V. A. Ioffe, and P. P. Feofilov, Opt. Spectrosc. **19**, 541 (1965).

[11] A. van Die, A. C. H. I. Leenaers, W. F. van der Weg, and G. Blasse, Mater. Res. Bull. **22**, 781 (1987).
[12] J. F. Donegan, T. J. Glynn, G. F. Imbusch, and J. P. Remeika, J. Lumin. **36**, 93 (1980).
[13] L. A. Riseberg and M. J. Weber, Solid State Commun. **9**, 791 (1971).
[14] U. Hömmerich, H. Eilers, W. M. Yen, and H. R. Verdun, Chem. Phys. Lett. **213**, 163 (1993).
[15] M. J. Weber and L. A. Riseberg, J. Chem. Phys. **55**, 2032 (1971).
[16] H. Kogelnik, Bell Syst. Tech. J. **48**, 2909 (1969).
[17] A. R. West, *Solid State Chemistry and its Applications* (Wiley, Chichester, 1984).